Synaptic kainate currents reset interneuron firing phase

Ellen J. Yang, Alexander Z. Harris and Diana L. Pettit

Department of Neuroscience, Albert Einstein College of Medicine, New York, NY 10461, USA

Hippocampal interneuron activity has been linked to epileptogenesis, seizures and the oscillatory synaptic activity detected in behaving rats. Interneurons fire at specific times in the rhythmic cycles that comprise these oscillations; however, the mechanisms controlling these firing patterns remain unclear. We have examined the role of synaptic input in modulating the firing of spontaneously active rat hippocampal interneurons. We find that synaptic glutamate receptor currents of 20–30 pA increase instantaneous firing frequency and reset the phase of spontaneously firing CA1 stratum oriens interneurons. Kainate receptor (KAR)-mediated currents are particularly effective at producing this phase reset, while AMPA receptor currents are relatively ineffective. The efficacy of KAR-mediated currents is probably due to their 3-fold longer decay. Given the small amplitude of the currents needed for this phase reset, coincident activation of only a few KAR-containing synapses could synchronize firing in groups of interneurons. These data suggest that KARs are potent modulators of circuit behaviour and their activation alters hippocampal interneuron output.

(Received 1 August 2006; accepted after revision 24 October 2006; first published online 26 October 2006)
Corresponding author D.L. Pettit: Department of Neuroscience, Albert Einstein College of Medicine, 1300 Morris Park Ave., K426, Bronx, NY 10461, USA. Email: dpettit@aecom.yu.edu

Synaptic hippocampal interneuron activity regulates the rhythmic and phasic activity of interneurons during cognition, sensory processing and exploratory behaviour (Cobb *et al.* 1995; Whittington *et al.* 1997; Klausberger *et al.* 2003; Whittington & Traub, 2003; Buzsaki & Draguhn, 2004). While the mechanisms responsible for generating and maintaining these varied rhythmic firing patterns remain unclear, a number of studies have suggested that synchronization of interneuron firing is critical (Traub *et al.* 1996; Whittington *et al.* 1997; Ermentrout & Kopell, 1998; Traub *et al.* 2004). For example, oriens lacunosum-moleculare (O-LM) and bistratified hippocampal interneurons fire at theta frequency (4–12 Hz) (O'Keefe, 1978; Traub *et al.* 2004), during the negative phase (at 19 ± 57 deg) of the field theta cycle rather than at random points throughout the cycle (Klausberger *et al.* 2003; Klausberger *et al.* 2004). Understanding the mechanisms responsible for generating this synchrony requires a better understanding of how interneuron firing is modulated.

A likely modulator of interneuron activity is the activation of kainic acid receptors (KARs). These receptors contribute to excitatory postsynaptic currents (EPSCs) at hippocampal pyramidal cells and interneurons (Castillo *et al.* 1997; Vignes & Collingridge, 1997; Cossart *et al.* 1998; Frerking *et al.* 1998; Mulle *et al.* 1998) and have been shown to produce profound effects on neuronal excitability. For example, exogenously applied kainate can synchronize neuronal networks (Fisahn *et al.* 2004; Traub *et al.* 2004), and induce seizures or epileptiform activity (Sloviter & Damiano, 1981; Westbrook & Lothman, 1983; Fisher & Alger, 1984; Ben-Ari, 1985). Consistent with these data, bath application of kainate modulates interneuron firing rates (Cossart *et al.* 1998; Frerking *et al.* 1998; Rodriguez-Moreno *et al.* 2000). Recent modelling of postsynaptic KAR activation suggested that KAR-mediated EPSPs tonically depolarize hippocampal interneurons (Frerking & Ohliger-Frerking, 2002). While these results are interesting, it remains unclear whether small amplitude KAR-mediated responses are sufficient to produce a change in firing rate, and further, whether this could have any role in altering the timing of interneuron output or synchronization.

We have examined the ability of small depolarizing currents to regulate the spontaneous firing of stratum oriens interneurons that project to CA1 pyramidal neurons. Synaptic and photolytic glutamate currents consistent with the activation of a few synapses were sufficient to increase instantaneous firing frequency. KAR-mediated currents were much more effective at modulating firing patterns than AMPA receptor-mediated currents. These differences in the efficacy of AMPAR and KAR currents are probably due to the slow KAR current decay, which we find is 3-fold longer than the decay of AMPAR currents. The increase in instantaneous firing frequency also produces a phase shift by restarting the firing pattern from the post-stimulus action potential (AP). This phase shift was independent of the time at

 DOI: 10.1113/jphysiol.2006.118448

which the depolarizing current was introduced within the AP firing sequence, suggesting that this phase shift is actually a phase reset of interneuron firing. A phase reset of interneuron firing could be a phenomenon by which input from a few principal neurons synchronizes groups of oriens interneurons firing out-of-phase.

Methods

Synaptic transmission

Animals were anaesthetized with trifluoroethane applied to gauze attached to the top of a closed chamber. This results in loss of consciousness within a minute. Animals were then decapitated in accordance with animal handling protocols approved by our institutional animal use committee. Coronal slices 300–400 μm thick were prepared from the hippocampus of P14–22 rats (Yang *et al.* 2006), and whole-cell recordings were made from stratum oriens interneurons. The patch pipette was filled with (mM): 135 $KMeSO_3$, 5 KCl, 1 $CaCl_2$, 5 EGTA, 10 glucose, 2 ATP, 0.3 GTP, 10 Hepes; pH to 7.2. Slices were superfused at 30°C with oxygenated physiological saline (mM: 119 NaCl, 2.5 KCl, 1.3 $MgCl_2$, 2.5 $CaCl_2$, 1 NaH_2PO_4, 26.2 $NaHCO_3$, 11 glucose). 4-methoxy-7-nitroindolinyl (MNI)-caged glutamate (200–500 μM) was added to the external solution (Tocris, Ellisville, MO, USA). Recordings were accepted only if the holding current was less than −150 pA when interneurons were voltage clamped at −70 mV. Current clamp recordings were terminated if the spontaneous firing became irregular. The regular, spontaneous and large-amplitude action potentials seen in the current clamp traces demonstrate cell health. Cells were electrically stimulated by placing a glass pipette electrode in the stratum oriens to activate synapses. Pure kainate receptor responses were isolated using GYKI 53655 (50–100 μM).

Photolysis

The output of a continuous emission 5 W krypton ion laser (Coherent, Innova 302) with a 351 nm line was delivered, via a multimode optical fibre, through an Olympus 40× water-immersion objective to form an uncaging spot (Wang & Augustine, 1995). An acousto-optical modulator was used to vary the duration of the light pulse between 0.200 and 2 ms. The uncaging spot was positioned over a cellular process by including a fluorescent dye (Oregon Green, 200 μM; Molecular Probes, Eugene OR, USA), in the patch pipette solution and then visualizing the cell with an Olympus Fluoview 300 confocal microscope. To avoid possible phototoxic affects, illumination was kept to a minimum. Optical images were taken of the filled cell and these images were then rendered off-line into a 3-dimensional reconstruction that was projected into two dimensions.

The size of the uncaging area was measured by photolysis of caged glutamate at 2 μm intervals along a line perpendicular to the dendrite using a motorized driver (MXMS-100i, SD Institute, Grants Pass, OR, USA). To calculate the size of the uncaging area, the peak amplitude of the current was plotted against uncaging position (relative to the dendrite) and fitted with a Gaussian function (see Supplemental Fig. 1). The width (5.7 μm) at half-maximal amplitude width was used as an estimate of uncaging spot size. The dendrite was positioned at the focal point of the uncaging beam by focusing up and down until a maximal response was achieved and sufficient time had elapsed to allow for receptor recovery from previous uncaging pulses (10 s). Electrophysiology data were collected and analysed off -line with Igor Pro (Wavemetrics, Lake Oswego, OR, USA).

Histology

To characterize interneuron morphology, neurobiotin (1%) was included in the pipette solution for all interneuron experiments. Slices were postfixed in 4% paraformaldehyde overnight at 4°C. After washing in PBS, slices were cryoprotected in 30% sucrose overnight and sectioned into 70 μm slices on a Leica CM3050 S cryostat. After air drying overnight on Fisher-plus slides (Fisher, Pittsburgh, PA, USA), sections were peroxidase quenched in 1% H_2O_2 (C.A.S. 7722-84-1, Acros Organics, New Jersey, USA). Neurobiotin was detected by incubating sections with an avidin–biotin–horseradish peroxidase complex (Elite ABC, Vector Laboratories, Burlingame, CA, USA). The horseradish peroxidase reaction was developed with 3,3′-diaminobenzidine tetrahydrochloride w/Co (D-0426, Sigma Fast, Sigma-Aldrich) (Pettit *et al.* 1999). After dehydration, sections were cleared in xylene, and coverslipped with Permount (Fisher). Morphological reconstructions were made with camera lucida using a 25× oil-immersion lens. Of the 61 cells examined in these studies 46 cells were filled with neurobiotin. From these 46, 26 cells were sufficiently filled to allow for identification of the axon termination. Cells were classified based on this termination as either oriens lacunosum-moleculare (O-LM; termination in lacunosum-moleculare), bistratified (termination in stratum radiatum), or trilaminar (termination in oriens and stratum pyramidale). We found 12 O-LM, 6 bistratified, and 8 trilaminar interneurons.

Results

Synaptic KAR currents can increase interneuron firing frequency

Previous work suggests that mixed AMPA–KAR, KAR-only and AMPAR-only excitatory inputs synapse onto

spontaneously firing horizontal CA1 interneurons at the oriens–alveus border (Cossart *et al.* 2002). As a result, we compared the relative efficacy of mixed AMPA–KAR and KAR currents in regulating interneuron firing patterns. Whole-cell recordings were obtained from these interneurons and a patch pipette-stimulating electrode was used to evoke synaptic currents. Only cells with regular firing patterns (coefficient of variance less than 0.3) were tested as large random changes in spike frequency and timing preclude analysis. AMPA–KAR responses were isolated by blocking NMDA (APV; 50 μM) and GABA (picrotoxin; 50 μM) receptors (Watkins, 1989; Yoon *et al.* 1993). To ensure that currents were physiologically relevant, stimulation was adjusted so that subthreshold AMPA–KAR synaptic currents (mean 20–40 pA; Fig. 1*A*) were recorded in voltage clamp (–70 mV). Once the stimulation intensity was calibrated, spontaneous APs were recorded in current clamp. A home-made timing device was used to trigger synaptic stimulation 50 ms after a detected AP. KAR-mediated synaptic currents were isolated by subsequent application of the AMPA receptor antagonist GYKI 53655 (GYKI; 50 μM) (Paternain *et al.*

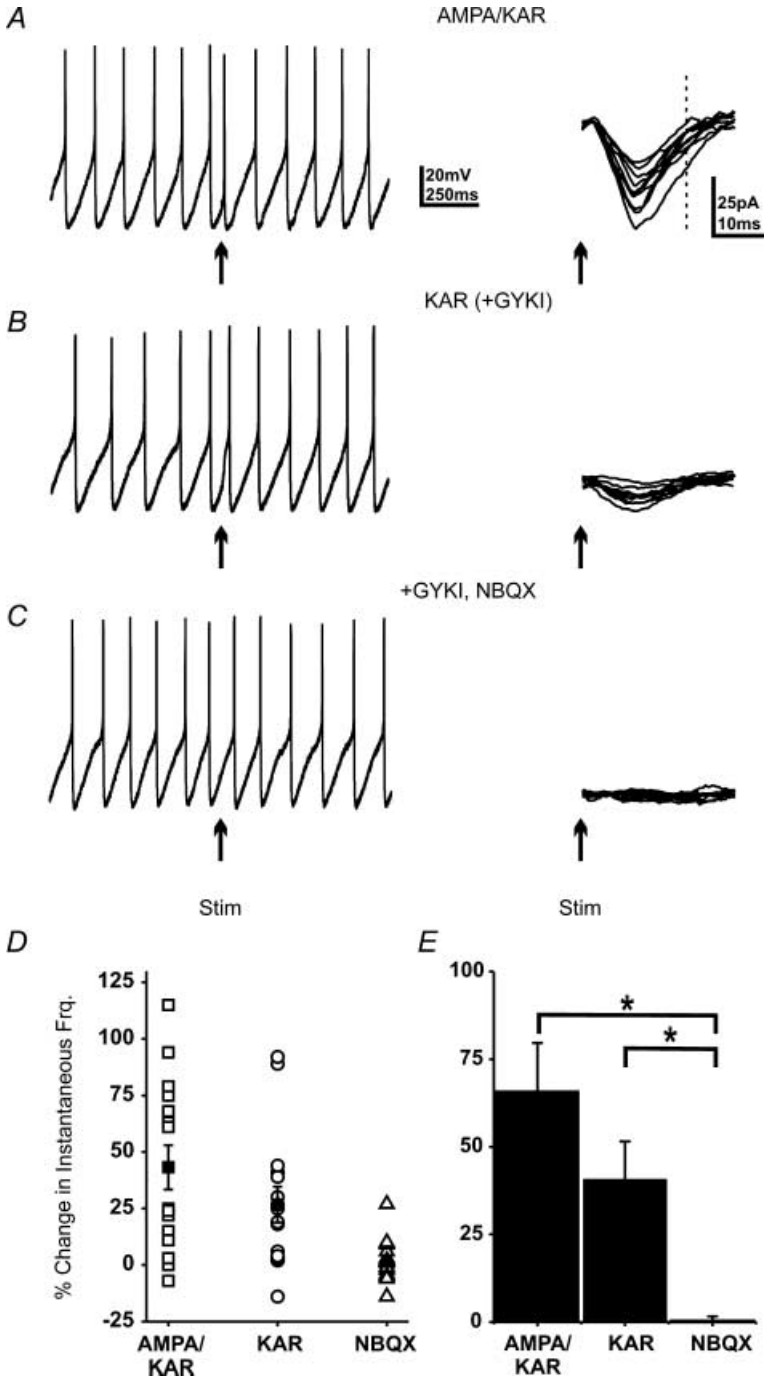

Figure 1. Single excitatory synaptic currents can increase spontaneous interneuron firing
A, a current clamp trace from a spontaneously firing interneuron and 15 consecutive voltage clamp traces of the synaptic current. Arrows indicate the time of stimulation; stimulus artifacts have been removed to better visualize small currents. Dashed line indicates timing of psAP. *B*, current and voltage clamp traces with AMPA receptors blocked to reveal the KAR-mediated current. *C*, after addition of NBQX (10 μM) electrical stimulation produced no synaptic current and no change in IFF. *D*, the change in IFF (15 consecutive trials) for each condition as shown in *A*–*C*. The mean increase was 43.2 $\pm$ 9.8% for mixed currents, 26.7 $\pm$ 7.8% for KAR currents and 1.7 $\pm$ 2.4% after NBQX application. *E*, average change in IFF across all cells. The increased IFF was statistically different from baseline for both currents (* ANOVA; $P < 0.0025$; $N = 5$).

1995; Huettner, 2003). Finally, KARs were blocked by adding NBQX (10 μM). The instantaneous firing frequency (IFF) was calculated for 15 consecutive trials by taking the inverse of the interspike interval for the post-stimulus AP (psAP). We found that these subthreshold currents advanced the timing of the action potential, transiently increasing IFF. This change was highly variable, consistent with the variability in current amplitude, averaging $43.2 \pm 9.8\%$ (Fig. 1*D*). Across all cells mixed AMPA–KAR currents increased IFF by $60 \pm 9.3\%$ ($N = 5$) of baseline following a synaptic current (Fig. 1*E*). The psAP did not coincide with the peak or rise of the synaptic current, confirming these currents were subthreshold (Fig. 1*A*, dashed line).

Subsequent block of the AMPA receptors reduced current amplitude by ~75% (4–12 pA; Fig. 1*B*); however, these small KAR currents also elicited an increase in IFF of $26.7 \pm 7.8\%$ ($N = 5$; Fig. 1*D*). Although the much smaller KAR currents produced less of an increase in IFF than the larger mixed currents, this difference was not statistically significant (ANOVA; $P > 0.05$). Application of NBQX blocked all current and any post-stimulus change in the firing pattern ($1.7 \pm 2.4\%$; Fig. 1*C*, *D* and *E*). While basal firing in these cells varied from 2.5 to 12 Hz, we saw no obvious frequency-dependent differences in the response to synaptic inputs. These data demonstrate that small synaptic currents can change interneuron firing patterns and that the KAR-mediated component is sufficient to produce much of the increase in IFF.

Kinetics of the KAR-mediated current

Due to the probabilistic nature of synaptic release, stimulation elicits currents of variable amplitude from synapses at unknown locations (Fig. 1*A*–*C*). In addition, the ongoing spontaneous firing of the cell obscures synaptic depolarization amplitudes, making it difficult to obtain thresholds or input–output relationships for the different current types. To address this problem, we used local photolysis of MNI-caged glutamate to elicit uniform currents at specified amplitudes (Pettit *et al.* 1997), and compiled input–output curves for AMPA *versus* KAR currents.

To allow for comparison between results obtained with synaptic stimulation and photolysis, we compared the decay and 10–90% rise times of synaptic and uncaging-induced EPSCs (uEPSCs). Previous work has suggested that synaptic and miniature KAR-mediated currents have slower rise and decay times than those of AMPAR-mediated currents (Frerking & Nicoll, 2000; Cossart *et al.* 2002; Huettner, 2003; Lerma, 2003). Mixed AMPA–KAR currents were elicited from whole-cell voltage-clamped (−70 mV) stratum oriens interneurons by placing a stainless-steel stimulating electrode in stratum oriens. Mixed AMPA–KAR responses were isolated by blocking NMDA (APV; 50 μM) and GABA (picrotoxin; 50 μM) receptors. Synaptic KAR responses were revealed by application of GYKI (50 μM) to block AMPARs. To obtain an estimate of the pure AMPAR-mediated synaptic current, an average of 50 consecutive KAR currents was subtracted from an average of 50 consecutive mixed currents (Fig. 2*A*). Current decay was measured by fitting the averaged traces with single exponentials (Fig. 2*A*). While mixed AMPA–KAR and KAR currents had similar decay time constants ($\tau = 11.2 \pm 0.8$ ms and $\tau = 13.4 \pm 0.7$ ms, respectively; $N = 9$), they were 3-fold slower than the AMPA current decay time constant ($\tau = 4.3 \pm 0.3$ ms; Fig. 2*B*; $P < 0.001$; ANOVA; $N = 9$). No significant differences were found in 10–90% rise times for synaptic currents before and after GYKI (50 μM) application (2.7 ± 0.6 and 3.0 ± 0.8 ms, respectively; $P > 0.05$; $N = 9$, paired Student's *t* test; Fig. 2*B*).

To obtain temporal measures of uEPSCs we used short photolytic pulses (200–500 μs; 500 μM MNI-caged glutamate; Tocris) to insure that photolysis was shorter than current rise time and minimize the time over which glutamate diffusion could occur. In addition to blocking NMDA (APV; 50 μM) and GABA (picrotoxin; 50 μM) receptors, voltage-gated Na^+ (TTX; 1 μM), K^+ (caesium) and Ca^{2+} (10 μM; cadmium) channels were blocked to prevent spontaneous activity and insure that all depolarizations were mediated by glutamate. In some experiments, saclofen (200 μM) and MCPG (1 mM) were added to block G-protein linked receptors ($N = 3$). Addition of these blockers had no effect on the kinetics of the currents. As with synaptic currents, AMPA receptors were blocked by application of GYKI (100 μM), unmasking the KAR-mediated current. GYKI blocked an average of $75.4 \pm 3.8\%$ of the total mixed AMPA–KAR current amplitude ($N = 10$). To compare the decay of the KAR uEPSC to the decay of a pure AMPA-mediated current, averages of three post-GYKI currents (KAR) were subtracted from an average of the pre-GYKI current (mixed AMPA–KAR; Fig. 2*C*). Comparison of the scaled currents revealed a much longer decay time for KAR currents (Fig. 2*D*). Exponential fits of the decays demonstrated that the average KAR current decay is over 3-fold longer ($\tau_{KAR} = 50.8 \pm 4.7$ ms; $\tau_{mixed} = 43.1 \pm 4.2$ ms) than the decay of subtraction (AMPA) currents ($\tau = 13.4 \pm 1$ ms). This difference in decay was statistically significant (Fig. 2*D*; $P < 0.001$, ANOVA; $N = 10$). Although previous work found no significant differences in the kinetics of AMPA and KAR uEPSCs (Eder *et al.* 2003), this may have been due to the lengthy uncaging times used in that study (3 ms). Under such conditions the large quantities of glutamate produced can diffuse to adjacent regions of dendrite, obscuring differences in decay time constants.

Comparison of the 10–90% rise times for uEPSCs before and after GYKI application showed that KAR currents

had slower rise times than mixed AMPA–KAR-mediated currents (Fig. 2*C* and *D*). The average 10–90% rise time for AMPA–KAR currents was 2.4 ± 0.1 ms while the rise time for KAR currents was 3.0 ± 0.2 ms. Although the difference was small, it represented a significant increase in rise time (Fig. 2*D*; $P < 0.005$; $N = 11$, paired Student's *t* test).

These results show that KAR uEPSCs have substantially longer (~3-fold) decays than synaptic EPSCs, and should also have larger charge transfer/peak current amplitude. As a result, the threshold for inducing a change in IFF with a uEPSC will be shifted to lower current amplitudes than those required for synaptic EPSCs. Given that mixed AMPA–KAR synaptic currents

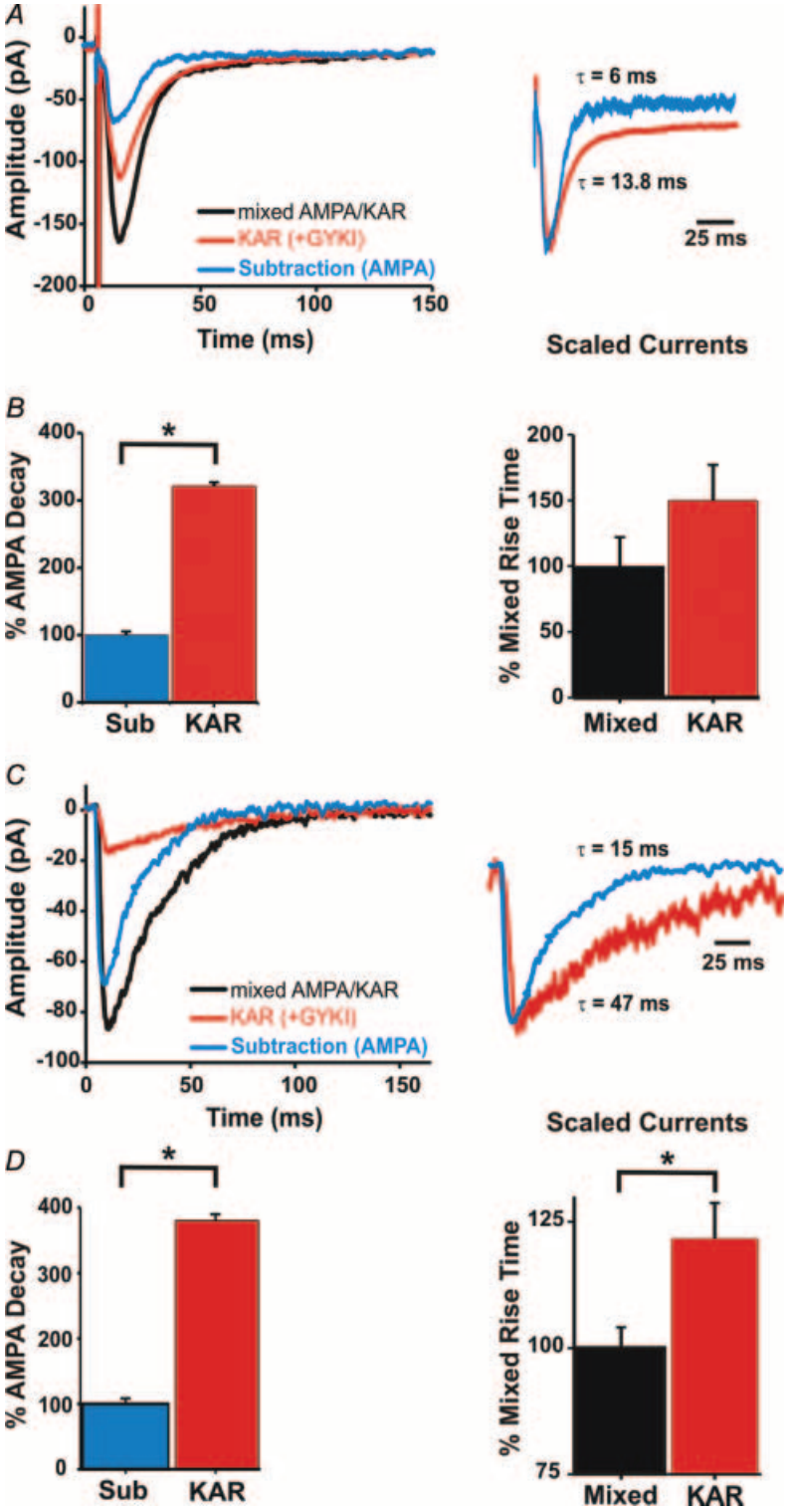

Figure 2. KAR-mediated currents have slower rise and decay times than AMPA receptor-mediated currents
A, whole-cell synaptic currents before (black) and after GYKI (50 μM; red) application. Subtraction of the KAR current from the mixed current yields an estimate of the AMPA current (blue). Traces are averages of 50 consecutive traces. Scaling the KAR current to match the subtraction (AMPA) current shows that the decay of the KAR current is slower. *B*, current decays were fitted with a single exponential. KAR decay is over 3-fold longer than the decay of the subtraction (AMPA) current. There was no significant difference in the 10–90% rise time ($P > 0.05$). Traces are averages of 50 consecutive trials. *C*, whole-cell photolytic currents from a stratum oriens hippocampal slice interneuron before (black) and after GYKI (100 μM; red) application. Subtraction of the mixed AMPA–KAR current from the GYKI current yields an estimate of the AMPA current (blue). Traces are averages of 3 trials. *D*, current decays were fitted with a single exponential. KAR decay is over 3-fold longer than the decay of the subtraction (AMPA) current. A plot of the change in 10–90% rise time shows a significant difference between KAR and mixed currents (* indicates significance; $P < 0.005$).

of 20–30 pA and synaptic KAR currents of 4–10 pA increase IFF, threshold uEPSCs are likely to be very small amplitude currents. It is important to note that the ratio of the AMPA/KAR decays were similar for both methods of activation (synaptic 3.21 *versus* uEPSCs 3.80), allowing us to use photolysis to differentiate between the effects of AMPA and KAR currents. Finally, photolysis allowed us to control current amplitude and generate input–output curves for mixed, KAR and AMPA currents.

KAR-mediated currents are more effective than AMPA-mediated currents at increasing firing frequency

We next compared the efficacy of AMPA *versus* KAR uEPSCs in the modulation of IFF. Glutamate currents were elicited by photolysis of MNI-caged glutamate (200 μM; 1 ms UV pulses). Current amplitude was measured in voltage clamp (−70 mV), and spontaneous AP firing was recorded by switching to current clamp. The cells were filled with fluorescent dye (Oregon Green-BAPTA 1, 200 μM; Molecular Probes), and confocal images were used to position the uncaging light beam (5.7 μm in diameter, see Supplementary Fig. S1) over the dendrites to generate active neurotransmitter (25–250 μm from the soma). To classify interneuron subtype, the internal solution also contained neurobiotin (1%) to allow for *post hoc* morphological analysis of dendritic location and axon terminations.

As with synaptic currents we compared the efficacy of photolytic AMPA–KAR, KAR and AMPAR currents at changing the IFF of the psAP. A single uncaging pulse was delivered 50 ms after a detected AP and subthreshold current amplitude was varied by changing either uncaging time or laser power. Following photolysis, any change in IFF was plotted against current amplitude. Figure 3*A* illustrates an individual cell where a depolarizing KAR current increased the IFF by 43.8 ± 5.1%, followed by a return to baseline upon decay of the current (Fig. 3*B*). Note that the psAP occurs after the uEPSC had decayed (Fig. 3*A*). Application of NBQX eliminated all photolytic

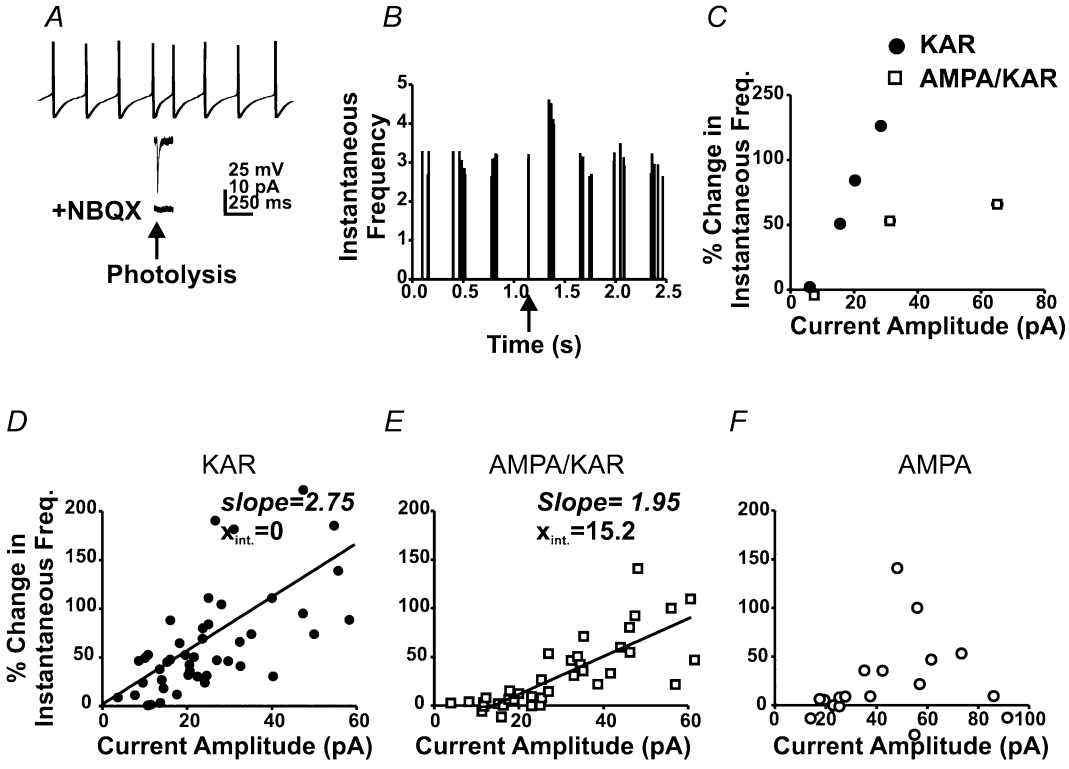

Figure 3. KAR-mediated currents are more effective than AMPA receptor-mediated currents at increasing spontaneous firing frequency in stratum oriens interneurons
A, current clamp trace of spontaneous APs from an interneuron before and after an uncaging pulse (arrow). Lower traces represent the KAR response to photolysis (middle), and following application of NBQX (10 μM; bottom). *B*, a plot of instantaneous firing frequencies for the interneuron in *A* (5 consecutive trials). The arrow indicates trigger AP. *C*, a plot of current amplitude *versus* change in IFF for both AMPA–KAR and KAR currents in a single interneuron. Current amplitude was varied by changing laser power while the uncaging delay was held constant at 50 ms. *D*, a plot of current amplitude *versus* the change in IFF for KAR currents for all cells ($N = 11$). *E*, current amplitude *versus* the change in IFF for mixed AMPA–KAR currents ($N = 9$). *F*, a plot of AMPA current amplitude *versus* change in frequency ($N = 5$).

current and any change in firing frequency in this cell (Fig. 3*A*).

KAR-mediated depolarizations

Dendritic KAR-mediated depolarizations were sufficient to increase IFF ($N = 11$). This change was independent of inhibition or activation of metabotropic glutamate receptors, as it was observed in the presence and absence of GABA and metabotropic receptor antagonists (PTX, 50 μM; MCPG, 1 mM; and MPPG. 500 μm; $N = 5$). To control for potential effects of UV light on firing rate, UV flashes were delivered in the absence of caged agonist; in this condition, firing rates remained unchanged ($N = 5$; data not shown).

Figure 3*C* illustrates the relationship between KAR and mixed AMPA–KAR current amplitude and the change in IFF within a single cell. A plot of current amplitude *versus* change in frequency before and after GYKI (50 μM) application demonstrates that KAR currents were more effective at producing an increase in IFF for all current amplitudes. Across all cells the smallest effective current amplitude observed was 4 pA which produced a 15% increase in frequency, while a 10 pA current produced a 50% increase (Fig. 3*D*; $N = 8$). These data indicate that small KAR depolarizations can effectively impact firing patterns.

Mixed AMPA–KAR-mediated depolarizations

Mixed AMPA–KAR currents were less effective as a function of peak amplitude than KAR currents at modulating interneuron firing rates ($N = 9$). Although mixed currents increased IFF, peak current amplitudes of 18 pA were required to obtain a 15% increase while currents of 38 pA produced a 50% increase (Fig. 3*E*). Since 75% of mixed current amplitude (Fig. 1) was due to AMPAR activation, an 18 pA mixed current contained approximately 4.5 pA of KAR current, which would also produce a 15% increase in IFF (Fig. 3*D*). These results indicate that the threshold for modulating IFF is shifted to higher peak current amplitudes for mixed AMPA–KAR currents. A linear regression fit of the pooled KAR (slope 2.75; $X_{\text{int}} = 0$; $N = 11$) and AMPA–KAR data (slope 1.95; $X_{\text{int}} = 15.2$; $N = 9$) further support a change in threshold. As shown in Fig. 3*C*, both KAR and mixed AMPA–KAR currents were tested in the same cells ($N = 4$) and results were in good agreement with between-cell comparisons.

When the charge transfer for mixed and KAR uEPSCs were plotted against their ability to change IFF, we found the minimum charge transfer required to achieve a 15% increase in IFF was approximately 200 pA ms (4 pA KAR; 18 pA mixed; Fig. 4*B*). We used this measure to estimate the size of mixed synaptic EPSCs needed to obtain a similar increase in IFF. A plot of synaptic current amplitude *versus* charge transfer shows that a mixed synaptic EPSP of ~25 pA would be necessary to obtain a similar charge transfer (Fig. 4*A*). This comparison is consistent with results from Fig. 1 in which similar synaptic currents produce a change in firing rate.

AMPA-only depolarizations

Finally, we examined the ability of pure AMPA-mediated currents to modulate firing frequency. As stated above, the effect of putative mixed AMPA–KAR *versus* KAR currents on IFF were sometimes compared in the same cell. Occasionally, we found interneurons in which no KAR-mediated currents could be elicited after GYKI application (Yang *et al.* 2006), indicating that the putative mixed currents were actually AMPAR-only currents ($N = 5$). This allowed us to examine AMPA currents independent of antagonists that may not be perfectly selective or commercially available. Pooled data from these cells were poorly fitted with a linear regression line because many cells did not respond, even at higher current amplitudes, while a few cells did show changes in firing rate

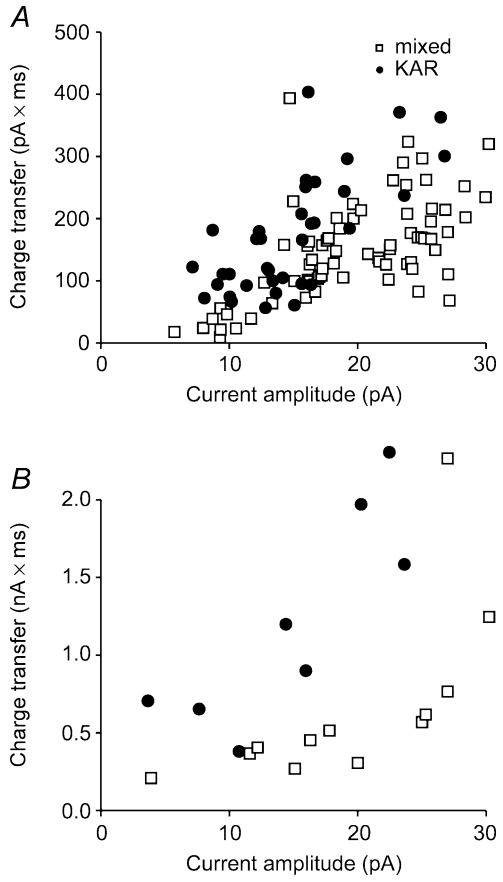

Figure 4. A plot of current amplitude *versus* charge transfer for KAR (●) and mixed currents (□)
A, a plot of charge transfer *versus* current amplitude for synaptic currents. *B*, a plot of charge transfer *versus* current amplitude for KAR and mixed uEPSCs shows that uEPSCs have a larger charge transfer/peak amplitude than synaptic EPSCs. The longer decay of the uEPSCs amplifies the charge difference between the two current types.

(Fig. 3*F*). Currents of ∼40 pA were required to obtain a 15% increase in IFF, and we estimated currents of ∼55 pA would be required to produce a 50% increase (Fig. 3*F*).

Neurobiotin fills of the interneurons tested in all of the above experiments revealed that they were oriens lacunosum-moleculare (O-LM; Fig. 5*B* and *E*), bistratified, and trilaminar cells (McBain *et al.* 1994; Sik *et al.* 1995; Freund & Buzsaki, 1996; Katona *et al.* 1999). Typical examples of live images, location of the uncaging beam, and the change in firing frequency for two O-LM interneurons are shown in Fig. 5*A*, *C* and *D*. Despite differences between the interneuron subtypes and basal firing rates (2.5–12 Hz), no subtype or frequency-dependent differences in the response to depolarizing currents were observed (see Supplementary material 2). These results demonstrate that inclusion of KARs at glutamatergic synapses can produce substantial modulations of cell excitability, effectively increasing the efficacy of the synapse.

The timing of glutamate currents predicts the magnitude of frequency change

By holding current amplitude constant and varying the length of the delay between the detected AP and the uncaging event, we were able to assess how timing of the KAR current affected the increase in spike frequency. Figure 6 illustrates results from an individual neuron in which the uncaging delay was varied from 1 to 200 ms. As in Fig. 2*A*, the psAP occured after the photolytic current had decayed (Fig. 6*B*). Maximal increases in IFF were obtained when the uncaging pulse occurred after the peak of the afterhyperpolarization (10–50 ms; Fig. 6*A* and *C*). Increases in IFF declined with longer delay times (in this cell > 100 ms) because a psAP cannot occur before the stimulus, e.g. the maximum possible IFF for a 200 ms delay is 5 Hz (Fig. 6*C*). Similar results were found for all cells tested, independent of their basal firing frequency ($N = 6$). Although KAR-mediated currents were tested in these experiments, comparable changes in frequency can be obtained with mixed AMPA–KAR currents of sufficient amplitude (Fig. 3*E*).

Small dendritic glutamate currents can shift the phase of interneuron firing

We have observed that stimulation often results in pairs of spikes in the firing pattern (Fig. 6*A*). These spike pairs could result from the introduction of an extra spike with

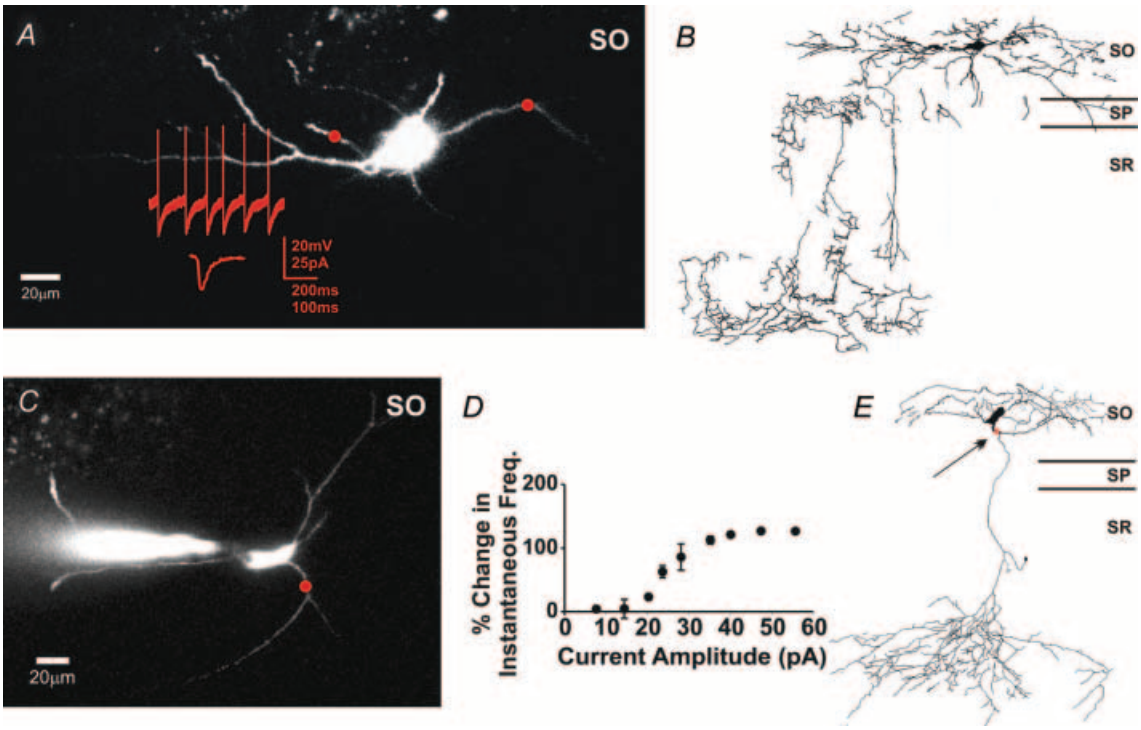

Figure 5. Morphological analysis of oriens interneurons
A, a live image of an interneuron with current and voltage clamp traces. The red circle represents the size and location of the photolysis area. Photolysis occurred 50 ms after the trigger action potential. *B*, a camera lucida drawing of the same cell as in *A*. The axon termination identifies it as an O-LM cell. *C*, another live image of an interneuron with a circle indicating the location of photolysis. *D*, a plot of current amplitude *versus* change in IFF for multiple mixed AMPA–KAR current amplitudes. Points are averages of 4 trials. *E*, a camera lucida drawing of the same cell as in *C*. The axon termination identifies it as an O-LM cell.

no change in the ongoing firing pattern (phase), or a restart of the firing pattern (phase shift) from the psAP. Since a phase shift would alter the timing of interneuron APs, such a shift could play a critical role in interneuron-mediated oscillations (Whittington & Traub, 2003; Traub *et al.* 2004). To resolve this question, we determined the IFF for the AP following the psAP. If the IFF returns to baseline, a phase shift has occurred. However, if IFF does not return to baseline, it would suggest that no phase shift has occurred. We found that the IFF returned to baseline (Figs 6*D* and 2*B*; $P > 0.25$, Student's t test, $N = 6$), indicating that a phase shift occurred.

To quantify the phase shift across all delays we calculated the average basal firing frequency for individual trials. This average interstimulus interval can then be used to predict when the next AP should occur. A graphical representation of the basal AP timing is shown as a sine wave in Fig. 7*A*. We then determined the actual time of each AP and subtracted

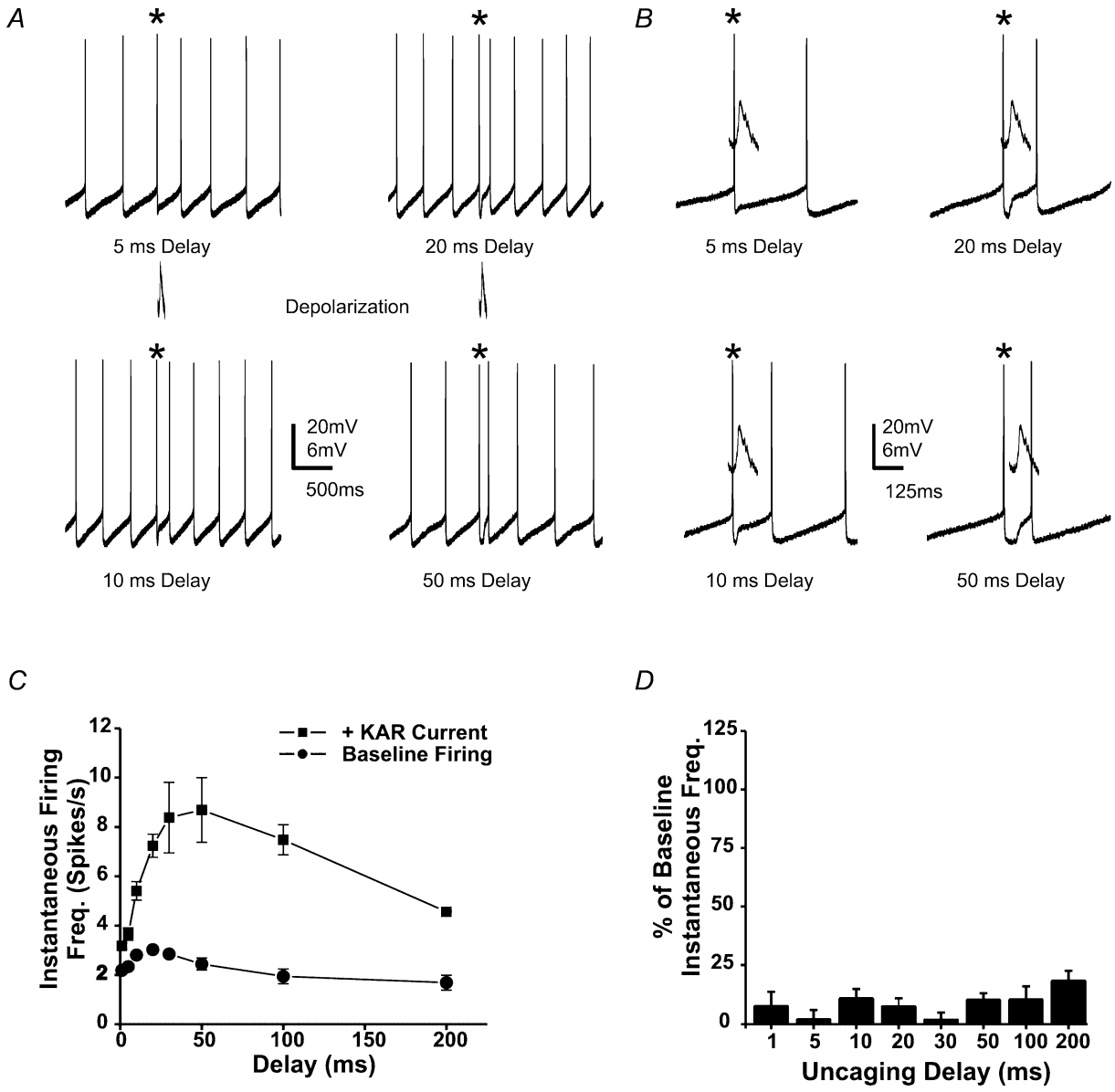

Figure 6. The timing of the glutamate current dictates the magnitude of the change in IFF
A, current clamp traces from a spontaneously firing stratum oriens hippocampal slice interneuron. The asterisks indicate the AP triggering an uncaging pulse. The photolytic pulse (1 ms) was delivered at varied delays from the trigger AP. *B*, an expanded time scale for traces in *A*. *C*, a plot of the KAR-mediated increase in IFF *versus* the delay from the detected spike for the cell in *A*. Firing frequency increased with increasing delays between spike and uncaging pulse. Baseline firing rates were calculated from the average of interspike intervals in the 1 s period before the uncaging. Individual data points represent averages of 4 consecutive trials. *D*, IFF returns to baseline for the second AP after the uncaging pulse.

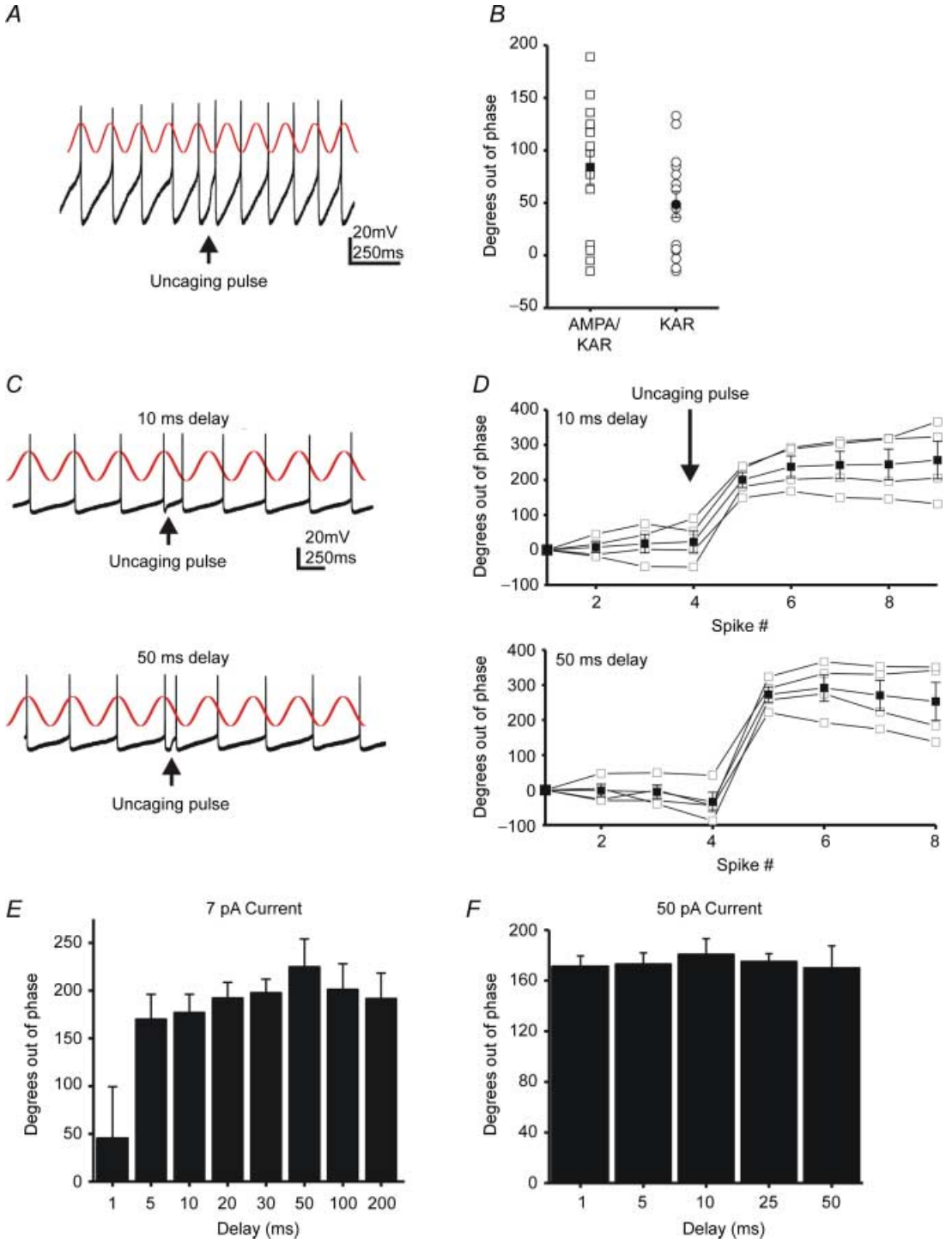

Figure 7. Single synaptic KAR currents can shift the phase of interneuron firing patterns
A, synaptic stimulation was delivered at the arrow (50 ms delay). An individual current clamp trace is superimposed on a sine wave of baseline firing frequency (from Fig. 1*B*). *B*, a plot of the phase shift for the cell in Fig. 1. 15 consecutive traces before and after GYKI application were measured. *C*, individual current clamp traces with a superimposed sine wave of baseline firing frequency. Photolysis occurred with a 10 ms or a 50 ms delay after the trigger AP. *D*, plots of the phase change or time differential between the expected spike and the predicted spike, as determined by the peak of the sine wave. The data are from the same cell in Fig. 4. The open squares are 4 individual trials, and the closed squares are the average. *E*, the average shift in phase for each uncaging delay in the same cell. Bars represent the shift of the first spike after the uncaging pulse. With the exception of the 1 ms delay, no significant differences were observed between delays ($P > 0.5$; Student's *t* test). *F*, a plot similar to that seen in *C* for a cell receiving a 50 pA photolytic current.

it from the predicted time. This difference was converted to degrees (time difference × (baseline interspike interval/360 deg)) to facilitate between-cell comparisons. To examine the ability of synaptic KAR currents to produce a phase shift we analysed 15 consecutive current clamp traces before and after application of GYKI (50 μM; $N = 5$). Consistent with our analysis of change in IFF following synaptic stimulation (Fig. 1), the phase changes varied significantly (Fig. 7*B*). While some traces showed no phase shift, others showed substantial shifts. On average, mixed currents produced larger shifts (100 ± 15 deg) than KAR currents (73 ± 12 deg) but this difference was not significant ($P > 0.05$; ANOVA). This suggests that the much smaller amplitude KAR currents were capable of inducing much of the phase shift. However, direct comparisons of input–output functions were hampered by the variance of synaptic depolarization amplitudes.

To further assess any differential effects of these currents, uEPSCs were also tested for their ability to change firing phase. Current amplitude was held constant while the photolysis delay was varied (Fig. 7*C* and *D*). As in Fig. 6 we found that the firing pattern shifted as a result of the psAP. We found that the 1 ms delay, which corresponds to a 15% increase in IFF, produced no phase shift (Fig. 7*E*). All other delays induced a phase shift that varied over 90 deg ($\pm$ 45 deg), a surprisingly small variance given that the stimulus was presented over delays encompassing 180 deg. As demonstrated in Fig. 3, current amplitude played a role in the magnitude of the increase in IFF. For small currents (< 25 pA, KAR), we frequently observed no phase shift for very short delays (1–5 ms), probably due to the large afterhyperpolarization at these time points. Larger currents (> 25 pA, KAR), on the other hand, were effective for all delays (Fig. 7*F*). These phase shifts were not accompanied by a change in the basal coefficient of variance for interspike intervals (baseline mean, 0.20; S.D., 0.05; range, 0.06–0.28; after stimulation mean, 0.21; S.D., 0.08; range, 0.08–0.3; sample size > 100 events per cell) after the uncaging current ($P > 0.5$, Student's t test, $N = 6$).

Despite the fact that KAR depolarizations lasted only milliseconds, they produced a phase shift which persisted for seconds (Fig. 7*D*). The duration of the phase shift depended on the magnitude of the shift and the basal variance of the cell. For example, the cell in Fig. 6*A* showing a smaller phase shift and more variance, returned to basal phase more quickly. These data suggest that subthreshold depolarizing currents advance the timing of the action potential, transiently increase IFF, and induce a phase change.

Small dendritic depolarizations reset the firing of oriens-alveus interneurons

Oriens interneurons participate in the production of oscillating rhythms; however, it remains unclear how glutamatergic inputs maintain the coherence of these oscillations. If excitatory inputs could cause interneurons firing out of phase to restart their firing pattern in unison, synchrony would be easy to achieve. In such a situation, the phase shift we observe would actually be a phase reset. In other words, no matter what the timing of the excitatory stimulus, a psAP occurs at a predicted time point following input. We tested this possibility by measuring the time interval between the stimulus and the psAP across all delays. For short delays (1–5 ms) we often saw small changes in IFF and no change in phase (Fig. 8*A* and *B*). The result was a long delay from the stimulus to the psAP. However, delays above 20 ms induced APs with very short delays so that the firing pattern was restarted, or reset to a restricted region of the firing cycle.

Since the baseline firing frequency of our cells ranges from 2.5 to 12 Hz, a 50 ms delay would occur at very different locations with the interspike interval for cells firing at 2.5 and 12 Hz. As a result, it was necessary to convert uncaging delay times to degrees, to allow for comparisons between cells. When the uncaging delay (in degrees) was plotted against the time to an psAP, the lag to the psAP for short delays (1–5 ms), was even more apparent (Fig. 8*C* and *D*; $N = 6$). However, stimuli arriving over the majority of a firing cycle (> 5 ms or 50 deg) produced APs within 15–20 ms. As a result, stimuli arriving over a large part of the firing cycle will produce APs with surprisingly similar time to the psAP across interneuron populations (Fig. 8*C* and *D*). This was true of all interneurons independent of their basal firing rates.

Within an individual cell, the phase shift varied an average of 90 ± 5.5 deg ($\pm$ 45 deg, Fig. 8*A* and *B*). This level of 'loose synchronization' is similar to that seen in recordings of hippocampal oscillations in which O-LM and bistratified interneurons fire during the negative phase of hippocampal oscillations $\pm \sim$60 deg (Klausberger *et al.* 2003, 2004). When stimuli arrived at the end of the cycle an AP also occurred within 15–20 ms. However, this AP was already at the end of the firing cycle and often failed to produce a phase shift. These data suggest that small depolarizing currents, comparable to the coincident firing of only a few synapses, can reset phase, and synchronize interneuron firing.

Given that synaptic currents have faster decays, we asked whether synaptic EPSPs were capable of inducing a phase reset. As we have already discussed, uEEPSPs arriving over a large portion of the firing cycle induced a psAP within 15–20 ms. If synaptic currents induced a psAP with a similar delay it would suggest that they can also reset firing phase. We measured time to the psAP for mixed synaptic currents (50 ms delay) which elicited at least a 30% change in IFF. The average delay to psAP was 17.2 ± 2.9 ms ($N = 5$ cells), confirming that synaptic and uEEPSPs have similar effects on spike timing.

Discussion

We found that subthreshold synaptic and photolytic glutamate currents corresponding to activation of only a few synapses (Ali & Thomson, 1998; Gloveli *et al.* 2004) were sufficient to increase the IFF of spontaneously firing stratum oriens interneurons. Given that unitary synaptic events in interneurons have been measured at 3–6 pA (Ali & Thomson, 1998; Gloveli *et al.* 2004), the coincident firing of 5–10 mixed AMPA–KAR synapses, would be enough to modulate firing. If there are KAR-only synapses on these interneurons, as suggested by previous work (Cossart

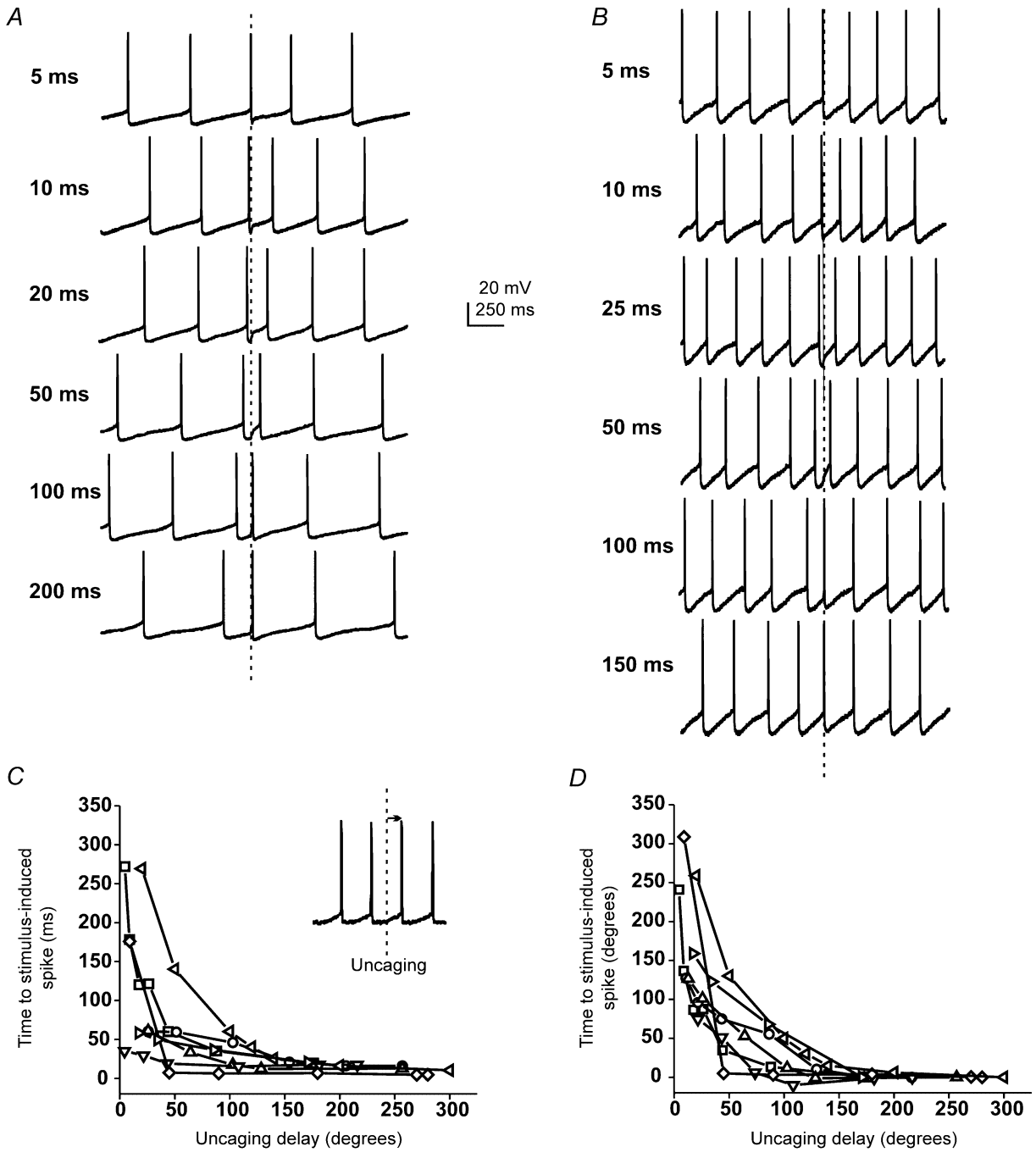

Figure 8. KAR-mediated currents reset the phase of interneuron firing
A, individual current clamp traces for a cell firing at 2.5–3 Hz. Traces are aligned from the time of photolysis (dashed line). *B*, current clamp traces for another cell firing at 4–5 Hz. *C*, a plot of the interval between the uncaging flash and the following AP *versus* uncaging delay ($N = 6$). *D*, the same data as in *A* with the time to spike plotted in degrees.

et al. 2002), fewer synapses may be required. In contrast, we found AMPA-only currents to be relatively ineffective as many of our AMPA-only cells failed to respond even to large amplitude currents (Fig. 3*F*). The reason for the increased efficacy of KAR-containing synapses was probably due to the 3-fold longer decay time relative to AMPA currents (13.4 *versus* 4.3 ms, respectively). Addition of KARs to the synapse significantly increased total charge, and provided a longer time window over which synaptic inputs can interact with neuronal pacemaker currents to produce an AP, increasing the efficacy of the synapse.

We did not investigate the ability of NMDA receptor (NMDAR) currents to modulate interneuron excitability. While we would expect that the long decay times of NMDAR currents would make them likely candidates for modulation, their contribution to small synaptic currents is usually only 10–15% due to receptor block by Mg^{+2}. For significant NMDAR activation to occur, substantial depolarization is necessary to remove that block. Under such conditions, the charge transfer carried by AMPA–KARs alone would be sufficient to produce an increase in firing frequency and excitability.

We have classified our experimental cells as O-LM, bistratified and trilaminar interneurons (McBain *et al.* 1994; Sik *et al.* 1995; Freund & Buzsaki, 1996; Cossart *et al.* 2006) based on dendritic and axon termination anatomy. We saw no obvious differences between these interneuron subtypes with respect to phase resetting by dendritic depolarizations. We have previously published data showing that the O-LM and trilaminar interneuron subtypes can express either high or low KAR densities (Yang *et al.* 2006). The majority of both cell types have KAR responses at the soma and all dendritic locations. Only a small minority show either no KAR currents or KAR currents restricted to a few dendritic spots. These cells appear healthy with respect to resting potential and have robust AMPAR-mediated currents. While these cells may represent a separate population of interneurons, their anatomy was indistinguishable from cells expressing KAR currents. Perhaps the distribution of KAR-mediated currents constitutes an additional dimension of hippocampal interneuron specialization.

Stratum oriens interneurons appear to have intrinsic properties that could provide a mechanism for the synchronization of interneuron firing observed during network rhythms and epilepsy. We saw no clear frequency-dependent differences as cells, with basal firing rates from 2.5 to 12 Hz responded in a similar fashion. While there may be subtle differences in threshold or sensitivity between these cells they all responded to synaptic inputs by changing spike timing and frequency. We have presented data suggesting that cells firing at similar rates could synchronize; however, it remains unclear how cells firing at very different basal rates might behave. Given that cells firing at 2.5 and 12 Hz both produced APs shortly after a synaptic input for a large portion of their firing cycle, it seems likely that these cells could synchronize briefly. However, subsequent APs would become more and more asynchronous. This problem is of course avoided if the synchronizing input is delivered at frequent intervals.

Experiments examining the firing patterns of oriens interneurons during theta waves show they fire at the most negative part of the cycle $\pm$ 60 deg (Klausberger *et al.* 2003, 2004). This produces a 'loose' synchrony which, while less than perfect, is sufficient to produce rhythmic activity. Our observed variability in phase change was $\pm$ 45 deg. This covered the entire range of time over which the psAPs occur, consistent with the requirements for rhythmic activity. Although we have focused on interneurons firing in the theta frequency, it is possible that synaptic depolarizations could also play a role in the synchrony necessary for gamma oscillations. Trilaminar interneurons that synapse in the perisomatic region play an important role in the synchronization of principal cell populations and the generation of gamma rhythms (Pike *et al.* 2000; Gloveli *et al.* 2004). In fact, hypersynchrony of these perisomatic cells may be a necessary precedent to the generation of seizures (Magloczky & Freund, 2005).

Stimuli which arrived over the majority of the firing cycle produced APs with surprisingly similar timing, while stimuli that arrived at the beginning and end of a cycle had very little effect. For two cells firing 180 deg out of phase to each other, the cell receiving input coincident with a spontaneous AP will not experience a shift in phase. However, the same stimulus will induce an AP within 10–20 ms in the cell firing out of phase. As a result the cells will now be firing in phase relative to each other. When larger groups of interneurons are considered, multiple rounds of input should produce a similar 'loose synchrony' within the population. Although electrical coupling through gap junctions may also contribute to interneuron synchrony (Perez Velazquez & Carlen, 2000), here we show a mechanism by which small synaptic currents may bridge groups of cells in interneuron network.

References

Ali AB & Thomson AM (1998). Facilitating pyramid to horizontal oriens–alveus interneurone inputs: dual intracellular recordings in slices of rat hippocampus. *J Physiol* **507**, 185–199.

Ben-Ari Y (1985). Limbic seizure and brain damage produced by kainic acid: mechanisms and relevance to human temporal lobe epilepsy. *Neuroscience* **14**, 375–403.

Buzsaki G & Draguhn A (2004). Neuronal oscillations in cortical networks. *Science* **304**, 1926–1929.

Castillo PE, Malenka RC & Nicoll RA (1997). Kainate receptors mediate a slow postsynaptic current in hippocampal CA3 neurons. *Nature* **388**, 182–186.

Cobb SR, Buhl EH, Halasy K, Paulsen O & Somogyi P (1995). Synchronization of neuronal activity in hippocampus by individual GABAergic interneurons. *Nature* **378**, 75–78.

Cossart R, Epsztein J, Tyzio R, Becq H, Hirsch J, Ben-Ari Y & Crepel V (2002). Quantal release of glutamate generates pure kainate and mixed AMPA/kainate EPSCs in hippocampal neurons. *Neuron* **35**, 147–159.

Cossart R, Esclapez M, Hirsch JC, Bernard C & Ben-Ari Y (1998). GluR5 kainate receptor activation in interneurons increases tonic inhibition of pyramidal cells. *Nat Neurosci* **1**, 470–478.

Cossart R, Petanjek Z, Dumitriu D, Hirsch JC, Ben-Ari Y, Esclapez M & Bernard C (2006). Interneurons targeting similar layers receive synaptic inputs with similar kinetics. *Hippocampus* **16**, 408–420.

Eder M, Becker K, Rammes G, Schierloh A, Azad SC, Zieglgansberger W & Dodt HU (2003). Distribution and properties of functional postsynaptic kainate receptors on neocortical layer V pyramidal neurons. *J Neurosci* **23**, 6660–6670.

Ermentrout GB & Kopell N (1998). Fine structure of neural spiking and synchronization in the presence of conduction delays. *Proc Natl Acad Sci U S A* **95**, 1259–1264.

Fisahn A, Contractor A, Traub RD, Buhl EH, Heinemann SF & McBain CJ (2004). Distinct roles for the kainate receptor subunits GluR5 and GluR6 in kainate-induced hippocampal gamma oscillations. *J Neurosci* **24**, 9658–9668.

Fisher RS & Alger BE (1984). Electrophysiological mechanisms of kainic acid-induced epileptiform activity in the rat hippocampal slice. *J Neurosci* **4**, 1312–1323.

Frerking M, Malenka RC & Nicoll RA (1998). Synaptic activation of kainate receptors on hippocampal interneurons. *Nat Neurosci* **1**, 479–486.

Frerking M & Nicoll RA (2000). Synaptic kainate receptors. *Curr Opin Neurobiol* **10**, 342–351.

Frerking M & Ohliger-Frerking P (2002). AMPA receptors and kainate receptors encode different features of afferent activity. *J Neurosci* **22**, 7434–7443.

Freund TF & Buzsaki G (1996). Interneurons of the hippocampus. *Hippocampus* **6**, 347–470.

Gloveli T, Dugladze T, Saha S, Monyer H, Heinemann U, Traub RD, Whittington MA & Buhl EH (2004). Differential involvement of oriens/pyramidale interneurons in hippocampal network oscillations *in vitro*. *J Physiol* **562**, 131–147.

Huettner JE (2003). Kainate receptors and synaptic transmission. *Prog Neurobiol* **70**, 387–407.

Katona I, Acsady L & Freund TF (1999). Postsynaptic targets of somatostatin-immunoreactive interneurons in the rat hippocampus. *Neuroscience* **88**, 37–55.

Klausberger T, Magill PJ, Marton LF, Roberts JD, Cobden PM, Buzsaki G & Somogyi P (2003). Brain-state- and cell-type-specific firing of hippocampal interneurons in vivo. *Nature* **421**, 844–848.

Klausberger T, Marton LF, Baude A, Roberts JD, Magill PJ & Somogyi P (2004). Spike timing of dendrite-targeting bistratified cells during hippocampal network oscillations in vivo. *Nat Neurosci* **7**, 41–47.

Lerma J (2003). Roles and rules of kainate receptors in synaptic transmission. *Nat Rev Neurosci* **4**, 481–495.

McBain CJ, DiChiara TJ & Kauer JA (1994). Activation of metabotropic glutamate receptors differentially affects two classes of hippocampal interneurons and potentiates excitatory synaptic transmission. *J Neurosci* **14**, 4433–4445.

Magloczky Z & Freund TF (2005). Impaired and repaired inhibitory circuits in the epileptic human hippocampus. *Trends Neurosci* **28**, 334–340.

Mulle C, Sailer A, Perez-Otano I, Dickinson-Anson H, Castillo PE, Bureau I, Maron C, Gage FH, Mann JR, Bettler B & Heinemann SF (1998). Altered synaptic physiology and reduced susceptibility to kainate-induced seizures in GluR6-deficient mice. *Nature* **392**, 601–605.

O'Keefe J & Nadel L (1978). *The Hippocampus as a Cognitive Map*. Oxford University Press, Clarendon.

Paternain AV, Morales M & Lerma J (1995). Selective antagonism of AMPA receptors unmasks kainate receptor-mediated responses in hippocampal neurons. *Neuron* **14**, 185–189.

Perez Velazquez JL & Carlen PL (2000). Gap junctions, synchrony and seizures. *Trends Neurosci* **23**, 68–74.

Pettit DL, Helms MC, Lee P, Augustine GJ & Hall WC (1999). Local excitatory circuits in the intermediate gray layer of the superior colliculus. *J Neurophysiol* **81**, 1424–1427.

Pettit DL, Wang SS, Gee KR & Augustine GJ (1997). Chemical two-photon uncaging: a novel approach to mapping glutamate receptors. *Neuron* **19**, 465–471.

Pike FG, Goddard RS, Suckling JM, Ganter P, Kasthuri N & Paulsen O (2000). Distinct frequency preferences of different types of rat hippocampal neurones in response to oscillatory input currents. *J Physiol* **529**, 205–213.

Rodriguez-Moreno A, Lopez-Garcia JC & Lerma J (2000). Two populations of kainate receptors with separate signaling mechanisms in hippocampal interneurons. *Proc Natl Acad Sci U S A* **97**, 1293–1298.

Sik A, Penttonen M, Ylinen A & Buzsaki G (1995). Hippocampal CA1 interneurons: an in vivo intracellular labeling study. *J Neurosci* **15**, 6651–6665.

Sloviter RS & Damiano BP (1981). On the relationship between kainic acid-induced epileptiform activity and hippocampal neuronal damage. *Neuropharmacology* **20**, 1003–1011.

Traub RD, Bibbig A, LeBeau FE, Buhl EH & Whittington MA (2004). Cellular mechanisms of neuronal population oscillations in the hippocampus in vitro. *Annu Rev Neurosci* **27**, 247–278.

Traub RD, Whittington MA, Stanford IM & Jefferys JG (1996). A mechanism for generation of long-range synchronous fast oscillations in the cortex. *Nature* **383**, 621–624.

Vignes M & Collingridge GL (1997). The synaptic activation of kainate receptors. *Nature* **388**, 179–182.

Wang SS & Augustine GJ (1995). Confocal imaging and local photolysis of caged compounds: dual probes of synaptic function. *Neuron* **15**, 755–760.

Watkins JC & GL (1989). In *The NMDA Receptor*, Chap 4. Oxford University Press, Oxford.

Westbrook GL & Lothman EW (1983). Cellular and synaptic basis of kainic acid-induced hippocampal epileptiform activity. *Brain Res* **273**, 97–109.

Whittington MA, Stanford IM, Colling SB, Jefferys JG & Traub RD (1997). Spatiotemporal patterns of gamma frequency oscillations tetanically induced in the rat hippocampal slice. *J Physiol* **502**, 591–607.

Whittington MA & Traub RD (2003). Interneuron diversity series: inhibitory interneurons and network oscillations in vitro. *Trends Neurosci* **26**, 676–682.

Yang EJ, Harris AZ & Pettit DL (2006). Variable kainate receptor distributions of oriens interneurons. *J Neurophysiol* **96**, 1683–1689.

Yoon KW, Covey DF & Rothman SM (1993). Multiple mechanisms of picrotoxin block of GABA-induced currents in rat hippocampal neurons. *J Physiol* **464**, 423–439.

Acknowledgements

This work was supported by NIH Grants 1RO1 NS44399, HD01799, DK07513, and the Whitehall Foundation. We would like to thank Drs Reed Carroll, Kamran Khodakhah and Lori McMahon for their helpful comments on the manuscript and Shennan Weiss for advice on data analysis.

Supplemental material

The online version of this paper can be accessed at:
DOI: 10.1113/jphysiol.2006.118448
http://jp.physoc.org/cgi/content/full/jphysiol.2006.118448/DC1
and contains one supplemental figure (measurement of the size of the uncaging area) and one table (basal firing frequency and change in IFF for a subset of interneurons).

This material can also be found as part of the full-text HTML version available from http://www.blackwell-synergy.com